Metabolic Characterization of Cellular Health Using a Multimodal Spectroscopy Technique

by

Eric Rosiek

A thesis submitted in partial fulfillment
of the requirements for the degree of
Master of Science in Engineering
(Bioengineering)
in the University of Michigan-Dearborn
2019

Master's Thesis Committee:

Associate Professor Nilay Chakraborty, Chair

Assistant Professor Amanda Esquivel

Assistant Professor Mathumai Kanapathipillai

TABLE OF CONTENTS

LIST OF FIGURES

ABSTRACT

The mitochondria act as a bridge between cell metabolism and overall cell health due to the dual roles it plays in both apoptosis and as the site of mitochondrial respiration. Using a combined analytical approach of extracellular flux analysis and Raman spectroscopy, studies and predictive estimations of cell health can be made through metabolism. Here, the protective effect of a D2/D3 agonist D512 is shown on the metabolism of oxidopamine treated neuronal origin cells (PC-12). D2/D3 dopamine receptor agnostic agents have been shown to alleviate symptoms of neurodegenerative diseases including Parkinson's disease in mouse models. It was observed that pre-incubation and co-incubation with D512 rescued metabolic parameters back to control levels. In addition, the effect of the bacterial quorum-sensing molecule 2-aminoacetophenone (2-AA) on RAW macrophage cells was studied. It was determined that at low concentrations (<200uM), 2-AA acted to increase mitochondrial metabolism, while at higher concentrations (>200uM), the metabolic rates decreased.

CHAPTER 1: INTRODUCTION

For cells moving through the cell cycle, there are two jobs that need to be performed. First one is expression of certain proteins to sustain the biochemical functions while the second being division of cells. For example, liver cells produce proteins that allow it to breakdown drugs or other xenobiotic compounds. Expressing protein, catalyzing replication of DNA, and dividing all require a tremendous amount of energy, which is derived from the biosynthesis of adenosine triphosphate (ATP) through metabolic pathways.

Healthy cells can respond quickly to times when high energy output is required. The increased energy requirement may also be required when cells sustain damage and attempt to repair themselves. If cells are unable to meet these increased energy demands, there exists an energy deficit. Cells in this state can undergo programmed cell death, called apoptosis (Fulda, 2014; Michael, 2016; Wang, 2009). Conversely, if a cell is undergoing apoptosis, metabolism will suffer, as the mitochondria are losing integrity (Orrenius, 2007). If protons are pumped across the inner mitochondrial membrane, fewer are passing through ATP synthase, and less ATP is generated. Once apoptosis has begun, the mitochondria reverse their polarity, releasing cytochrome c. This begins a cascade where caspases are released, and they begin breaking down the cell (Porter, 1999). Thus, characterization of cellular damage from the point of view of metabolic output and chemical analysis can be potentially indicative of failures in cellular process.

Currently, there exist many methods to study metabolism *in vitro* (Simmonet, 2014; Teslaa, 2014). Though they are non-destructive, conventional fluorescent tags are bulky molecules and could possibly affect the microenvironment of a given cell. For example, certain dyes like those of the MitoTracker product line permanently bind with the mitochondria (Chazotte, 2011). This could modify the mitochondria and lead to measurements that are distorted. Traditional fluorescent probes are only useful as an endpoint

assay. Most interactions between fluorescent molecules and their substrates are irreversible, which causes an inability to measure future states of the cells. Two non-destructive and non-disruptive methods will be used to measure metabolism: extracellular flux analysis and Raman microspectroscopy (Mookerjee, 2018; Pelletier, 2014). Extracellular flux analysis is a fluorescence spectroscopy technique which uses solid state fluorescent probes to characterize the extracellular environment of a given cell sample. Extracellular environments have been shown to be similar to intracellular environments, and thus measurements of metabolism using extracellular flux analysis can be associated with the metabolism inside the cell (Mo, 2009). The fluorophore in a solid state probe does not enter the cell, thus it is much less disruptive to the cells, and the data acquired is more realistic.

Raman spectroscopy allows for spatial and temporal characterization of metabolites in the cells. It uses the properties of inelastic scattering of light to identify certain bonds that are associated with metabolites that are of importance to metabolism. Every bond motion scatters light differently, which allows for identification of functional groups in the cell. Unlike IR-spectroscopy, samples can be in aqueous states, which allow imaging of biological samples.

For the purpose of this project, the metabolic health of two cell types will be determined under various *in vitro* conditions. In chapter two, the protective effect of D512 will be studied in PC-12 cells that have been incubated with the neurotoxin 6-hydroxydopamine. D512 is part of a class of molecules that have agonistic action against the dopamine receptors D2 and D3. Previously, many treatments for Parkinson's have been shown to act as agonists to these two receptors. 6-hydroxydopamine generates an oxidative environment as it breaks down, thus it generates a cell model of the Parkinson's disease state. As stated previously, there is a link between metabolism and overall cell health. Measurements of metabolic properties will be made for various treatments of D512 to determine if D512 can protect metabolism in cells treated with 6-hydoxydopamine.

In chapter three, the effects of 2-aminoacetophenone on RAW cells will be determined. When bacteria invade a host, a host-pathogen relationship is formed. Pathogens must walk a thin line between surviving and being detected in the host. If the pathogen disrupts immune cells, a stronger immune response

may be generated by the host. Without any protection from the immune system, the pathogen will be quickly dispatched. The opportunistic bacterium *p. aeruginosa* is a common bacteria associated with the frequent infections seen in the lungs of cystic fibrosis patients. It *uses* quorum sensing to modulate its gene expression, and to change how its colonies behave once established in the host. 2-aminacetophenone is one of the molecules it uses for quorum sensing, and it has been shown to both aid in and disrupt how hosts deal with pathogens. Study of the effect of 2-aminoacetophenone on metabolism in RAW 264.7 macrophages will illuminate how this specific pathogen interacts with hosts.

This multimodal spectroscopy technique will determine a variety of metabolic parameters, from which, larger claims about overall cell health can be made.

CHAPTER 2: PROTECTION OF METABOLIC FUNCTION BY D2/D3 AGONIST D512

Neurodegenerative diseases affect a large portion of the elderly, with the most common being Alzheimer's disease and Parkinson's disease. In both of these diseases, loss of dopaminergic neurons is seen, and is thought to be the cause of each disease's typical symptoms. In Alzheimer's the loss of neurons occurs most notably in the cortex, while in Parkinson's this loss is seen in the substantia nigra (Bhat, 2015). The substantia nigra controls reward and movement, and neuronal loss here leads to the typical motor afflictions seen in patients with Parkinson's. Mood disorders and cognitive decline are also attributed to this loss (Adler, 2005). Though it is unclear how these cells are lost, it is thought that apoptosis and oxidative stress play roles (Cadenas, 2000; Cohen, 1997; Singh, 2007). Oxidative environments have been previously shown to negatively impact cells due to changes in DNA and proteins, in addition to lipid oxidation. Under oxidative conditions, dopamine is converted to 3,4-Dihydroxyphenylacetic acid (DOPAC), which then could be reacted with hydrogen peroxide to generate more oxidative metabolites (Pires, 1992). Oxidation of L-DOPA, a precursor of dopamine, also produces free radicals (Basma, 1995; Lotharius, 2002).

Oxidopamine (6-OHDA) allows for the study of this oxidative environment in dopaminergic cell models. Through the oxidation of dopamine, 6-OHDA can be produced (Linert, 2000). 6-OHDA autoxidizes to produce hydrogen peroxide, which then generates an oxidative environment both intracellularly and extracellularly (Blum, 2000; Gee, 1989; Saito, 2007). This

leads to both necrosis and apoptosis in dopaminergic cells (Hanrott, 2005). Exposure to 6-OHDA causes Parkinson's symptoms in mice (Blum, 2001; Breese, 2005).

The PC12 cell line is derived from rat pheochromocytoma, and serves as a model cell for dopaminergic neurons (Greene, 1982; Shafer, 1991). The purpose of this experiment is to measure metabolic parameters for the potential treatments of a novel D2/D3 agonist D512 (Pre-Incubation, Pre/Co-Incubation), and compared them to the positive control and negative control (6-OHDA). The D2 and D3 receptors are dopamine receptors that, when bound to, will inhibit formation of cAMP through inhibition of adenyl cyclase. (Neves, 2002; Usiello, 2000) These two receptors have been shown to be targets for novel compounds that offer treatments for Parkinson's (Biswas, 2008; Glennon, 2006; Gogoi, 2011; Jones, 2010; Joyce, 2007; Millian, 2010). D512 not only binds with the D2/D3 receptors, but it has the ability to scavenge free radicals, which in turn lessens the effects of oxidative stress on the cell (Johnson, 2012).

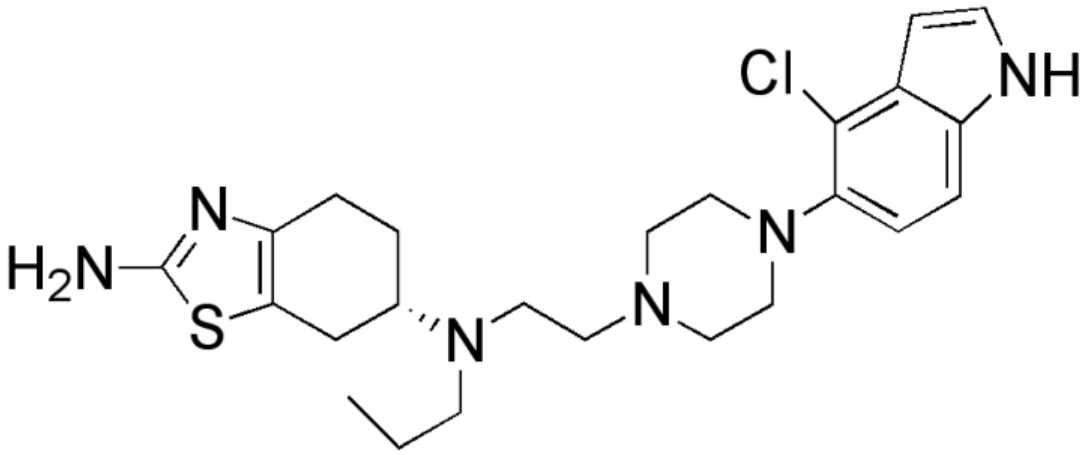

D-512

Figure 1: Structure of D512

Since D512 has already been shown to prevent apoptosis in *in vitro* cell samples, it is expected that either Pre-Incubation or Pre/Co-Incubation will counter the effect of 6-OHDA, and rescue metabolic parameters to the levels seen in the control condition (Shah, 2014). If only the Pre/Co-Incubation succeeds in rescuing the metabolic parameters, it will indicate that the effects of D512 on the cells are not long-lasting.

Metabolic parameters will be measured using extracellular flux analysis. Extracellular flux analysis allows for non-destructive, real time measurement of mitochondrial and glycolytic activity. Conventional assays for measuring metabolism are destructive or disruptive, and only yield what is essentially a basal measurement of activity at a set time. Agilent's Seahorse xFp Extracellular Flux Analyzer use solid-state fluorescent probes to measure both oxygen level and pH over short periods of time (Moura, 2014). From these measurements Oxygen Consumption Rate (OCR), and extracellular acidification rate (ECAR) are calculated. OCR corresponds to mitochondrial activity, as oxygen is converted to water when electrons are passed to complex IV of the electron transport chain (Kadenbach, 1987). ECAR is a measure of glycolytic activity due to a proton leaving the inorganic phosphate when it binds to adenosine diphosphate (ADP) to form adenosine triphosphate (ATP). Each condition of cells was subjected to a mitochondrial stress test, and a glycolysis stress test. Sample mitochondrial and glycolytic tests are included in the appendix.

In addition to these metabolic measurements, measurements of growth will also be collected, to indicate if D512 can improve growth rate in cells treated with 6-OHDA.

Raman spectroscopy will be used to measure phenylalanine to CH_2 ratios, as phenylalanine plays an important role in catecholamine synthesis (Wang, 2014). Some change is expected in cells undergoing apoptosis. Raman spectroscopy is a vibo-rotational spectroscopy method that is

reliant on inelastic scattering of light (Stavely, 2016). Each bond, when scattering light inelastically, will rotate or vibrate in some way, releasing lower energy light than what initially struck the bond. This shift is called Stokes-Raman scattering, each bond motion has its own specific shift. This allows for fingerprinting of molecules, like in IR spectroscopy. However, unlike in IR spectroscopy, Raman spectroscopy allows for imaging of solutions, which is the form most biological molecules are in. Ratios can be made of the wavenumbers of the light that returns, and that can indicate comparable concentrations of desired bond in each treatment. It is worth noting that Raman spectroscopy is non-destructive and non-perturbing, allowing for a more realistic, cell by cell measurement of each condition. A sample Raman spectrum of a simple trehalose in water system is shown in the appendix.

Materials and Methods

Cell culture and treatments

Cells were cultured in T-25 flasks (Thermo Fisher Scientific, Waltham, MA) and maintained in RPMI 1640 (Gibco) medium supplemented with 10% heat-inactivated horse serum (Gibco), 5% fetal bovine serum (Gibco), 100U/mL penicillin, and 100ug/mL streptomycin at 37°C in 95% air/5% CO2. Stock solutions of D-512 and 6-hydroxydopamine were prepared in DMSO and aliquots were stored at −20°C and −80°C, respectively. For all experiments assessing neuroprotective effects of D-512, the treatment conditions are as follows: D512 alone, 6-OHDA alone, D512 then 6-OHDA, and D512 then D512/6-OHDA. All treatments are 24hr incubation with either 10 μM D512 and/or 75 μM 6-OHDA. These concentrations were optimized by Shah et al. in their previous work[Shah].

Treatments	Incubation
Control	24hr media
D512	24hr 10uM D512
6-OHDA	24hr 75uM 6-OHDA
Pre-Incubation	24hr 10uM D512, then 24hr 75uM 6-OHDA
Pre/Co-Incubation	24hr 10uM D512, then 24hr 10uM D512 and 75uM 6-OHDA

Table 1: List of Conditions

Metabolic Analysis

Analysis of metabolic function for both conditioned and control cells were carried out on an extracellular flux analyzer (XFp Seahorse, Agilent Technologies, Santa Clara, CA). All Seahorse consumables were purchased from Agilent. Cells were trypsinized and counted using trypan blue exclusion. Cells were seeded in prescribed microwell plates at a seeding density of 10^4 cells per well. After 24 hr incubation, the media was replaced with conditioned media and the plates were incubated for 24 hr more. Both oxygen consumption rate (OCR) (representing mitochondrial respiration) and extracellular acidification rate (ECAR) (representing glycolysis) measurements were taken using standard Seahorse protocol, following optimization, with N=3. Briefly, xFp cartridge sensors were hydrated and injection ports loaded by the following; mitochondrial test reagents used oligomycin (1 μM), carbonyl-cyanide-4-(trifluoromethoxy) phenylhydrazone (FCCP, 0.5 μM), and rotenone/antimycin A (0.5 μM). Glycolysis test reagents used D-glucose (10 mM), oligomycin (1 μM), and 2-deoxyglucose (2-DG, 50 mM). All reagents have corresponding final concentrations in cell chambers immediately after being listed. Oligomycin was used as the F_0F_1-ATPase inhibitor and oxygen consumption rates measured in presence of this inhibitor indicate proton leak. FCCP acts as an uncoupling agent that collapses

the mitochondrial proton gradient and thereby uncouples oxidation from phosphorylation, maximizing oxygen consumption rates. The contribution of energy generation via non-mitochondrial processes was quantified in relation to the overall oxygen flux using rotenone and antimycin A. Rotenone and antimycin A inhibit complex I and III, respectively, of the respiratory system. Glucose was supplied as to fully saturate basal ECAR. Then, since oligomycin inhibits ATP synthase in the electron transport chain, ATP/ADP ratio decreases, which stimulates glycolysis. 2-DG is a glucose analog which competitively inhibits hexokinase, effectively arresting glycolysis.

Measurement of cell viability

To determine the neuroprotective effect of D-512 on 6-OHDA-mediated cell death, a long-term viability study was performed. PC12 cells were plated in T-25 flasks at approximately 2.5x10 cells/flask density in 5 mL media and allowed to grow for 24hr. Cells were treated with each of the treatment conditions, then were removed to fresh media. Cells were collected using trypsinization followed by centrifugation. A hemocytometer (Hausser Scientific, Horsham, PA) was used to count live cells using Trypan Blue exclusion technique. Cells were enumerated on days 1 and 3 with N=4.

Raman microspectroscopy

Spatially correlated Raman microspectroscopic measurements were employed to characterize living PC-12 cell samples in in-vitro culture conditions. A customized confocal microscope (Zeiss Corp., Germany) and Raman spectrometer combination (UHTS 300, WITec Instruments Corp., Germany) was used and the Raman spectra were collected using an EMCCD camera (Andor Technology, UK) at a spatial resolution of 500 nm. A 532 nm solid state laser calibrated to 20 mW was used for excitation and a

custom 50X high resolution objective (Mitutoyo, Japan).

The changes in the spectral signature from the intracellular space were analyzed using a hyperspectral molecular analysis technique. Raman spectral arrays were acquired for neurofibroma cells. Hyperspectral maps were collected using a spatial dimension of 40μm×40μm with a spectral dimension of 80x80 pixels, with N=3. Each array of scans was collected using an integration time of 0.5 s. Principal component analysis (PCA) was used to reduce the dimensionality of the collected spectral data arrays into principal components (PCs). A non-linear iterative partial least squares algorithm was used for related vector analysis to eliminate noise in the spectral baseline. Following noise reduction using PCA, hierarchal cluster analysis was used to construct an average spectral signature for the cells.

Statistical analysis

Data are expressed as mean value ± standard error mean (SEM). For multiple groups, statistical significance was determined using one-way analysis of variance (ANOVA) following Tukey's Multiple Comparison post hoc test. In all cases $P < 0.05$ was considered as statistically significant.

Results

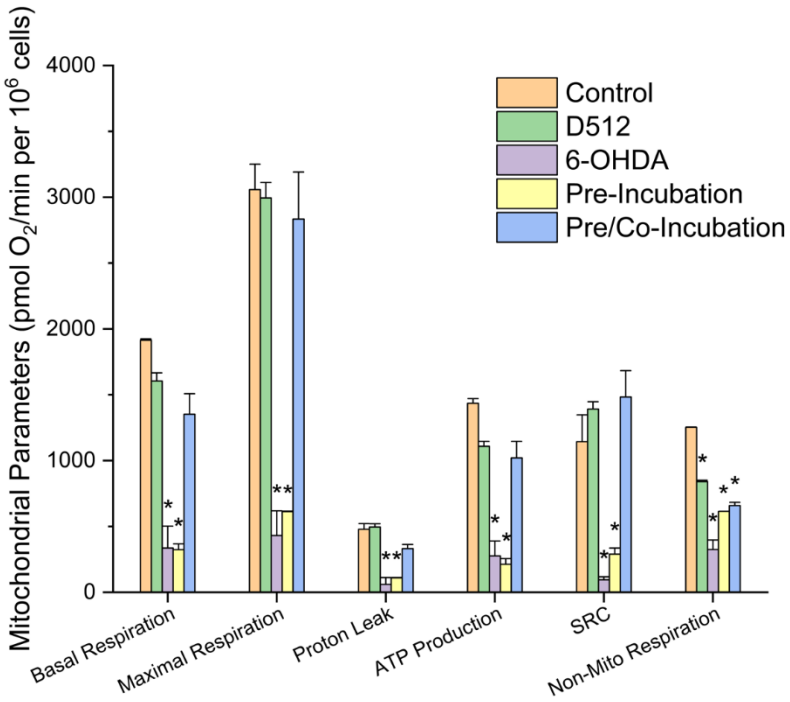

Figure 2: Mitochondrial Parameters of treated PC-12 from Mitochondrial Stress Test

Mitochondrial Parameters were calculated using formulae present in the Agilent's Mito Report Generator Guide. Values were normalized by number of cells in each well to yield values per million cells. *<0.05 against control. Error is +/- SEM, n=3.

In Figure 2, Mitochondrial Parameters are shown. Briefly, all measurements for each condition had the respective non-mitochondrial respiration subtracted from them to normalize. Maximal respiration is the value of OCR after addition of FCCP, a mitochondrial uncoupling agent. Spare respiratory capacity (SRC) is calculated as maximal respiration minus basal respiration. ATP Production is calculated as the difference between basal OCR and minimum OCR after oligomycin is added. The difference between the minimum OCR after oligomycin addition, and the minimum OCR after rotenone addition is the proton leak. This describes the protons that are not passing through ATP synthase when pumped across the membrane by Complexes I, III and IV Pre and Co incubation with D512 in addition to 6-OHDA rescues mitochondrial parameters

to control levels. D512 alone had no effect on any mitochondrial parameters except for non-mitochondrial respiration. A ~70% decrease in all parameters was seen in cells only pretreated with D512 and in cells that were treated with 6-OHDA alone.

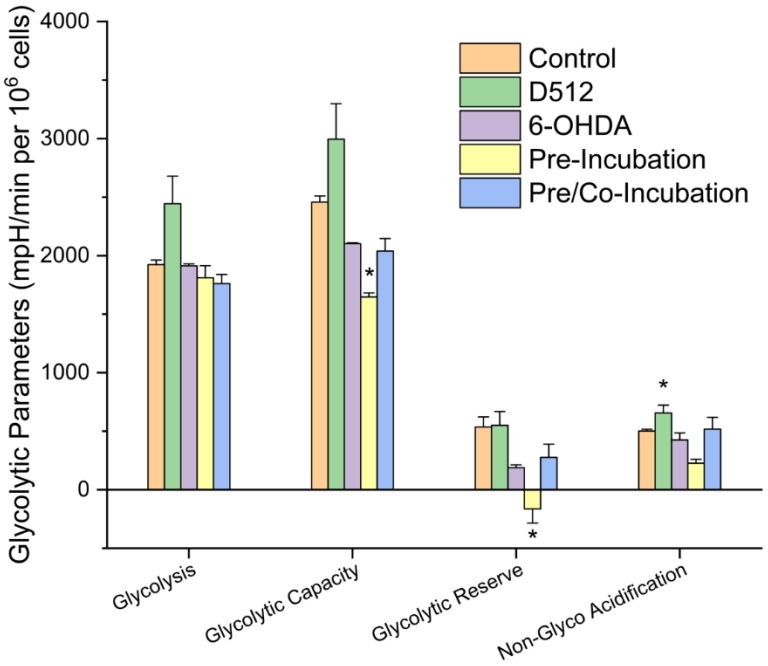

Figure 3: **Glycolytic Parameters of treated PC-12 from Glycolytic Stress Test**

Glycolytic Parameters were calculated using formulae present in the Agilent's Glyco Report Generator Guide. Values were normalized by number of cells in each well to yield values per million cells. *<0.05 against control. Error is +/- SEM, n=3.

In Figure 3, Glycolytic Parameters are shown. Briefly, non-glycolytic acidification is the ECAR value upon addition of 2-DG, which halts glycolysis. Acidification due to basal glycolysis is maximum ECAR upon addition of glucose minus non-glycolytic acidification. Glycolytic Capacity is the maximum ECAR value after addition of oligomycin minus non-glycolytic acidification. Glycolytic Reserve is Glycolytic Capacity minus Glycolysis. Glycolytic

parameters were non-significantly elevated in cells treated with D512 alone. Cells treated with D512 alone also had a significantly higher non-glycolytic acidification. No significant differences in glycolytic parameters were seen for both Pre/Co-incubated cells and cells treated with 6-OHDA alone when compared to control. Significant differences from control are seen in Glycolytic Capacity and Glycolytic Reserve for Pre-incubated cells.

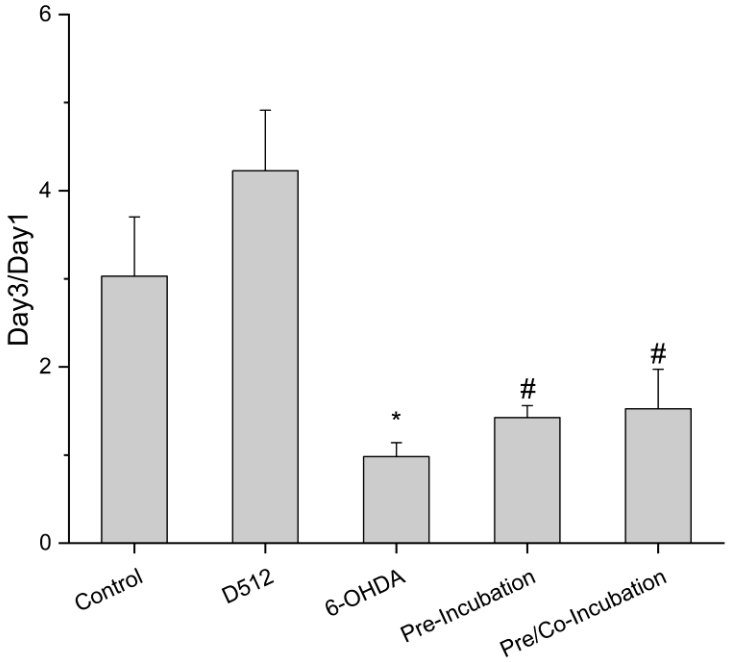

Figure 4: Growth Rate between days 1 and 3

The ratio between the number of cells on day 3 and the number of cells on day 1 is shown. *<0.1 against control and D512. #<0.1 against D512. Error is +/- SEM, n=4.

As seen in Figure 4, Cells treated with 6-OHDA had a ratio of close to 1, indicating no growth in this time. Both pre-incubation and pre/co-incubation had lowered growth when compared to control. D512 treated cells had a non-significantly higher growth rate than control.

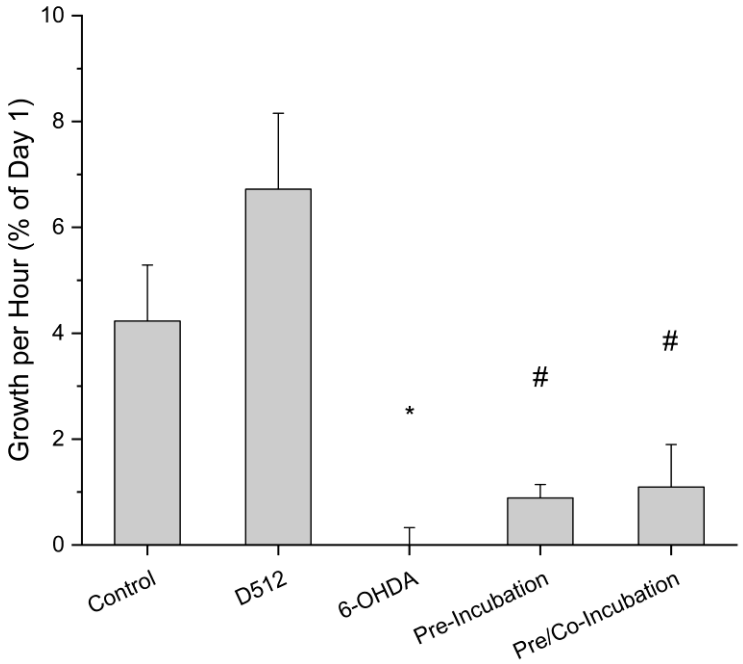

Figure 5: Growth Rates of Conditioned PC-12

Difference in cell number between day 1 and day 3 was divided by 48 hours to generate a linearized growth per hour parameter for each condition. These parameters were the normalized by their respective day 1 counts to yield growth per hour as a percentage of day 1 for each condition. *<0.1 against control and D512. #<0.1 against D512. Error is +/- SEM, n=4.

Like seen in Figure 4, Figure 5 shows that 6-OHDA treated cells had almost no growth. Growth rates were increased ~60% from control in cells incubated with D512 alone. Growth rates in the treatment conditions are non-significantly higher than 6-OHDA, but are still ~75% lower when compared to control.

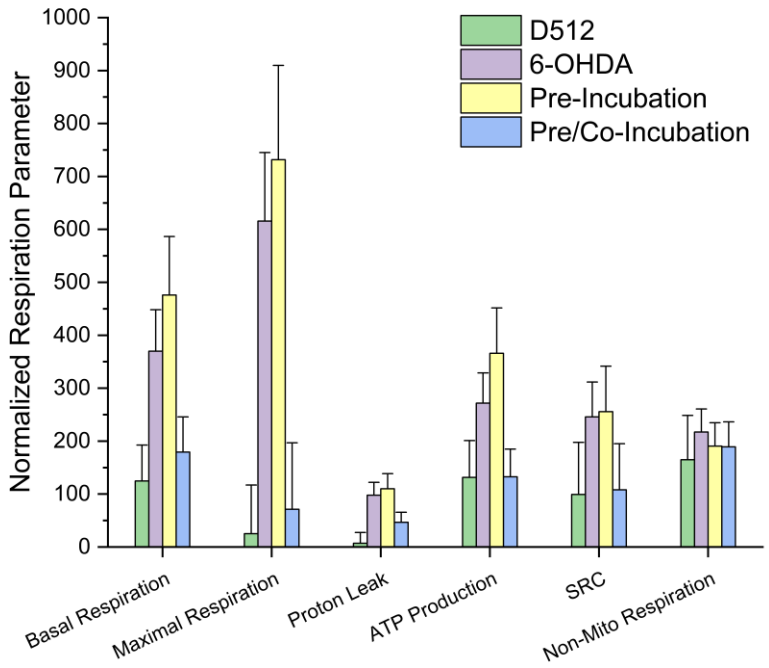

Figure 6: Normalized Respiration Parameters for treated PC-12

The difference of each parameter from control was calculated for each treatment. These values were then normalized by the change in growth rate from control for each respective treatment. The absolute value of the ratio of these differences is presented here. Error is +/- SEM, n=3.

For Figure 6, a higher value for normalized respiration parameter indicates higher correlation with change in growth rate for that treatment. Pre-Incubation and 6-OHDA have changes in mitochondrial parameters that have high correlations to their respective changes in growth rate. Pre/Co-Incubation has little change from control in terms of mitochondrial parameters, but has a lower growth rate, leading to a smaller normalized respiration parameter than Pre-Incubation or 6-OHDA.

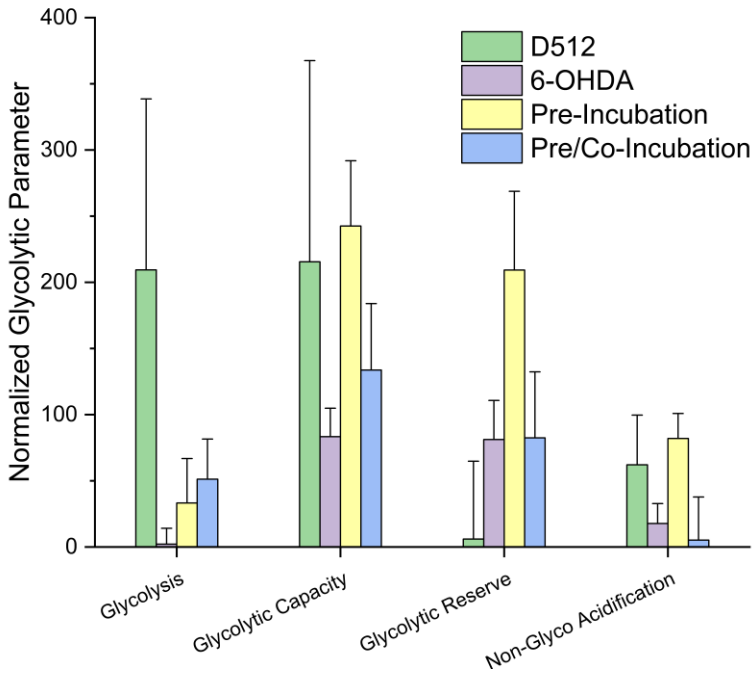

Figure 7: Normalized Glycolytic Parameters for treated PC-12

The difference of each parameter from control was calculated for each treatment. These values were then normalized by the change in growth rate from control for each respective treatment. The absolute value of the ratio of these differences is presented here. Error is +/- SEM, n=3.

Similar to Figure 6, in Figure 7, a higher value for normalized glycolytic parameter indicates higher correlation with change in growth rate for that treatment. Most notably, the value is high for D512 for Glycolysis and Glycolytic Capacity. Both growth and these respective parameters are increased from the control condition.

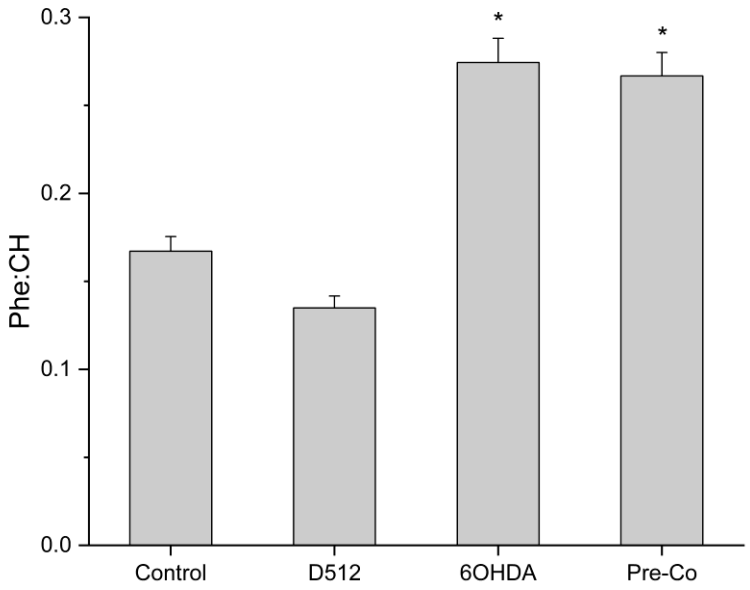

Figure 8: Ratio of Phenylalanine Spectral Intensity CH_2 Spectral Intensity

Ratios are of the intensity of the 1004cm^{-1} peak to the intensity of the 2940cm^{-1}. *<0.05. Error is +/- SEM. N=3.

In Figure 8, the 1004cm^{-1} is the peak associated with phenylalanine, and 2940cm^{-1} is associated with presence of organic molecules. Higher phenylalanine to organic compound ratios are seen in cells treated with 6-OHDA in some form. A slight non-significant decrease in phenylalanine to CH_2 ratio is seen in D512 when compared to control.

Discussion

Glycolytic parameters are not changing significantly in any condition when compared to control, though cells treated with D512 alone had slightly elevated glycolytic parameters compared to control cells. D512 treated cells also have unchanged mitochondrial parameters when compared

to control. This indicates that D512 causes an extra energy demand, and the cells are addressing this demand through increased glycolytic activity.

Mitochondrial parameters are significantly lower in cells treated with 6-OHDA. This aligns with what has been seen in previous studies when PC-12 cells are exposed to 6-OHDA (Shah, 2014). The mitochondria of these cells have most likely begun apoptosis, and they have lost integrity (Hanrott, 2005).

Mitochondrial and glycolytic parameters for the Pre/Co-Incubated condition are not statistically significant, indicating that a pre/co-incubation of D512 with 6-OHDA negates the apoptosis-inducing effect of 6-OHDA. This protective effect has been seen before in the work by shah et al.

The difference seen between pre-incubation and pre/co-incubation shows the impermanence of the effect of D512 on PC-12 cells.

Growth rate is slightly elevated in PC-12 cells treated with D512. As seen in figure 6, this increase in growth is well correlated to the increase in glycolytic parameters seen. This stimulation of growth could explain the increased energy demand the cells are under, which then the cells make up for by increasing glycolytic activity.

Growth rate is severely depressed in 6-OHDA treated cells. This aligns with the high correlation seen in figure 5. These cells are likely apoptotic, and this can be seen through both metabolism and growth (Hanrott, 2005; Orrenius, 2007). Pre-treated cells also have this high correlation between depressed mitochondrial parameters and depressed growth.

Pre/Co-incubated cells had a low correlation between mitochondrial metabolism and growth as seen by the decreased growth coupled with no change in mitochondrial parameters. This shows

that even though the cells are metabolizing properly, the energy from this metabolism is not being used for growth, but more likely repair. The cells must repair damage from the 6-OHDA before growth rates are restored

Phenylalanine plays an important role as an intermediate in the synthesis of signaling molecules like dopamine and epinephrine. From Figure 9, and increase in phenylalanine with respect to organic material indicates higher phenylalanine concentrations in cells treated with 6-OHDA in any form. This could be showing a failure in the pathways used to synthesize signaling molecules.

Conclusion and Further Work

This study confirms the anti-apoptotic effect of D512 seen by Shah et al. Though pre/co-incubation with D512 protected the metabolism, growth rate post treatment was still depressed when compared to control. This is indicative of non-mitochondrial oxidative damage that is cause by 6-OHDA, and this damage must be repaired before growth returns.

The failure of pre-incubation to protect the cells from apoptosis shows the timescale on which D512 is acting. The effect of D512 is not permanent, which allows for controllability should this drug be used as a treatment for Parkinson's disease. D512 alone also had no adverse effects when compared to control cells.

Raman spectroscopy analysis offers another method to differentiate the treated cells. Phenylalanine is an important precursor in the reactions needed to produce dopamine and epinephrine. As PC-12 cells are dopaminergic, they react to signaling molecules, and produce them. An increase is seen between conditions that were treated with 6-OHDA in any form, and

those that were not. Cells treated with 6-OHDA may have damage done to this pathway, and as a result, phenylalanine could be accumulating.

Further studies can be run on increased concentrations of D512 to determine if growth rates can be rescued in 6-OHDA treated cells. Further characterization of potential oxidative damage can also be done.

CHAPTER 3: EFFECT OF QUORUM SENSING MOLECULE 2-AMINOACETOPHENONE ON METABOLISM IN RAW 264.7 MURINE MACROPHAGE CELLS

When a bacterium invades a host, a complex relationship is formed, commonly known as the host-pathogen relationship. Both host and pathogen are modifying their gene expression, trying to defend themselves against the other side. This change in gene expression is frequently found in the opportunistic bacterium *Pseudomonas aeruginosa* (Olizer, 2000; Parsek, 1999; Whiteley, 2001). *P. aeruginosa* causes many of the lung infections that are typical in patients suffering from cystic fibrosis, and approximately 46% of patients test positive for PA (Cystic Fibrosis Annual Report, 2017). *P. aeruginosa* uses a quorum sensing system to determine when to expresses certain genes while its bacterial colony is expanding. Quorum sensing is a signaling pathway where unless a certain population of bacteria is reached, certain genes will be expressed (Miller, 2001). *P. aeruginosa* releases 2-aminoacetophenone (2-AA) as a quorum sensing molecule. 2-AA is formed as one of many quorum sensing molecules (Kim, 2009).

It has been shown that pre-treatment with 2-AA before infection with *P. aeruginosa* improves survival of mice *in vivo* (Bandyopadhaya, 2012). It has also been shown that 2-AA disrupts mitochondria in skeletal muscle (Tzika, 2013). This ebb and flow between the immune system and the bacteria is commonly seen when studying the host-pathogen relationship.

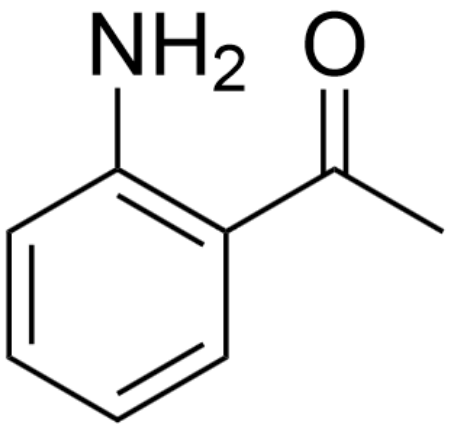

Figure 9: Structure of 2-aminacetophenone

The purpose of this study is to examine the effect that 2-AA might have on the metabolism of RAW 264.7 murine macrophages. Due to the results of the previous studies on the effect of 2-AA, some change in metabolism is expected. Metabolism not only powers growth, and new protein synthesis, but it also provides energy for existing proteins to perform their functions. Whether presence of 2-AA signals macrophages to divide, to make protein, or to generate ATP in anticipation of increased demand, changes should be seen in metabolism (James, 1995). These changes will reveal the relationship between 2-AA and metabolism in RAW macrophages.

A synthesis of extracellular flux analysis and Raman microspectroscopy will be used to study metabolism.

Metabolic parameters will be measured using extracellular flux analysis. Extracellular flux analysis allows for non-destructive, real time measurement of mitochondrial and glycolytic activity. Conventional assays for measuring metabolism are destructive or disruptive, and only

yield what is essentially a basal measurement of activity at a set time. Agilent's Seahorse xFp Extracellular Flux Analyzer use solid-state fluorescent probes to measure both oxygen level and pH over short periods of time (Moura, 2014). From these measurements Oxygen Consumption Rate (OCR), and extracellular acidification rate (ECAR) are calculated. OCR corresponds to mitochondrial activity, as oxygen is converted to water when electrons are passed to complex IV of the electron transport chain (Kadenbach, 1987). ECAR is a measure of glycolytic activity due to a proton leaving the inorganic phosphate when it binds to adenosine diphosphate (ADP) to form adenosine triphosphate (ATP). Each condition of cells was subjected to a mitochondrial stress test, and a glycolysis stress test. Sample mitochondrial and glycolytic tests are included in the appendix.

In addition to the Mito and Glyco Stress Test, a Real-Time ATP Assay will conducted on the conditioned RAW cells. This helps to determine how much ATP is produced per cell, and where the ATP is coming from. The conditions of the Real-Time ATP Assay are more similar to growth conditions. Sample curves for OCR and ECAR during the ATP Test are included in the appendix.

Raman spectroscopy will be used to study the ratio of NADH to organic molecules in RAW cells incubated with various concentrations of 2-AA. Raman spectroscopy is a vibo-rotational spectroscopy method that is reliant on inelastic scattering of light. Each bond, when scattering light inelastically, will rotate or vibrate in some way, releasing lower energy light than what initially struck the bond. This shift is called Stokes-Raman scattering, each bond motion has its own specific shift. This allows for fingerprinting of molecules, like in IR spectroscopy. However, unlike in IR spectroscopy, Raman spectroscopy allows for imaging of solutions, which is the form most biological molecules are in. Ratios can be made of the wavenumbers of the

light that returns, and that can indicate comparable concentrations of desired bond in each treatment. It is worth noting that Raman spectroscopy is non-destructive and non-perturbing, allowing for a more realistic, cell by cell measurement of each condition. A sample Raman spectrum of a simple trehalose in water system is shown in the appendix.

Materials and Methods

Cell culture and treatments

RAW 264.7 cell lines were purchased from American Type Culture Collection (ATCC® TIB-71™). Cells were cultured in T-25 flasks (Thermo Fisher Scientific, Waltham, MA) and maintained in DMEM (Gibco) supplemented with 10% fetal bovine serum (Gibco), 4mg/mL L-glutamine, 100U/mL penicillin, and 100ug/mL streptomycin at 37°C in 95% air/5% CO2. All conditioning with 2-AA was performed as a 24hr incubation with the desired concentration of 2-AA.

Metabolic Analysis

Analysis of metabolic function for both conditioned and control cells were carried out on an extracellular flux analyzer (XFp Seahorse, Agilent Technologies, Santa Clara, CA). All Seahorse consumables were purchased from Agilent. Cells were trypsinized and counted using trypan blue exclusion. Cells were seeded in prescribed microwell plates at a seeding density of $5x10^3$ cells per well. After 24 hr incubation, the media was replaced with conditioned media and the plates were incubated for 24 hr more. Both oxygen consumption rate (OCR) (representing mitochondrial respiration) and extracellular acidification rate (ECAR) (representing glycolysis) measurements were taken using standard Seahorse protocol, following optimization. Briefly, XFp cartridge sensors were hydrated and injection ports loaded by the following; mitochondrial test reagents used oligomycin (1 μM), carbonyl-cyanide-4-(trifluoromethoxy) phenylhydrazone

(FCCP, 0.5 μM), and rotenone/antimycin A (0.5 μM). Glycolysis test reagents used D-glucose (10 mM), oligomycin (1 μM), and 2-deoxyglucose (2-DG, 50 mM). The Real-Time ATP Assay used oligomycin (1.5 μM), and rotenone/antimycin A (0.5 μM). All reagents have corresponding final concentrations in cell chambers immediately after being listed. The ATP Assay used N of 6, while the mitochondrial and glycolytic stress tests used N of 3.

Oligomycin was used as the F_0F_1-ATPase inhibitor and oxygen consumption rates measured in presence of this inhibitor indicate proton leak. FCCP acts as an uncoupling agent that collapses the mitochondrial proton gradient and thereby uncouples oxidation from phosphorylation, maximizing oxygen consumption rates. The contribution of energy generation via non-mitochondrial processes was quantified in relation to the overall oxygen flux using rotenone and antimycin A. Rotenone and antimycin A inhibit complex I and III, respectively, of the respiratory system. Glucose was supplied as to fully saturate basal ECAR. Then, since oligomycin inhibits ATP synthase in the electron transport chain, ATP/ADP ratio decreases, which stimulates glycolysis. 2-DG is a glucose analog which competitively inhibits hexokinase, effectively arresting glycolysis.

Raman Microspectroscopy

Spatially correlated Raman microspectroscopic measurements were employed to characterize living RAW 264.7 cell samples in in-vitro culture conditions. Cells were incubated in various concentration of 2-AA for 24hr, then imaged. A customized confocal microscope (Zeiss Corp., Germany) and Raman spectrometer combination (UHTS 300, WITec Instruments Corp., Germany) was used and the Raman spectra were collected using an EMCCD camera (Andor Technology, UK) at a spatial resolution of 500 nm. A 532 nm solid state laser calibrated to 20 mW was used for excitation and a custom 50X high resolution objective (Mitutoyo, Japan).

The changes in the spectral signature from the intracellular space were analyzed using

a hyperspectral molecular analysis technique. Raman spectral arrays were acquired for macrophage cells. Hyperspectral maps were collected using a spatial dimension of 40μm×40μm with a spectral dimension of 80x80 pixels, with N of 3. Each array of scans was collected using an integration time of 0.5 s. Principal component analysis (PCA) was used to reduce the dimensionality of the collected spectral data arrays into principal components (PCs). A non-linear iterative partial least squares algorithm was used for related vector analysis to eliminate noise in the spectral baseline. Following noise reduction using PCA, hierarchal cluster analysis was used to construct an average spectral signature for the cells.

Statistical analysis

Data are expressed as mean value ± standard error mean (SEM). For multiple groups, statistical significance was determined using one-way analysis of variance (ANOVA) following Tukey's Multiple Comparison post hoc test. In all cases $P < 0.05$ was considered as statistically significant.

Results

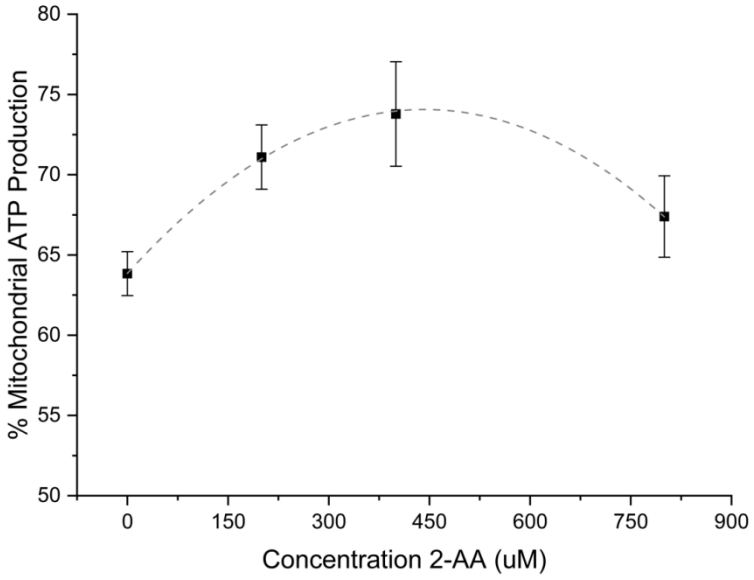

Figure 10: Mitochondrial ATP Production as a share of total ATP Production for treated RAW cells

OCR and ECAR measurements were converted to mitochondrial ATP production and glycolytic ATP production, respectively, using the equations found in the ATP Assay Report Generator. These equations can be found in the appendix.

An increase in share of ATP produced from mitochondrial respiration is seen in cells incubated in lower concentrations (<400uM) of 2-AA. A decrease in percentage of ATP from mitochondrial respiration is seen when concentration of 2-AA is increased from 400uM to 800uM.

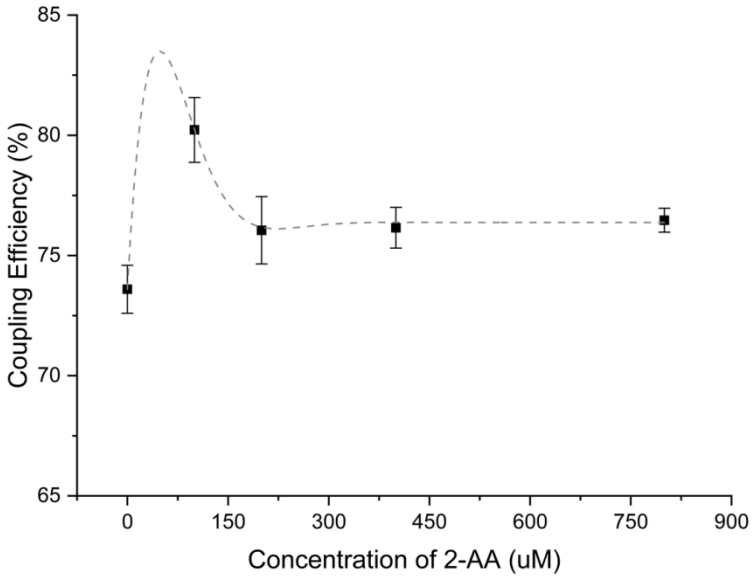

Figure 11: Coupling Efficiency of treated RAW cells

Coupling Efficiency is used to measure how intact the inner mitochondrial membrane is for a given condition. It measures how many protons return through ATP Synthase after being pumped across the membrane by Complexes I, III and IV.

Though an increase in Coupling Efficiency is seen in cells treated with 100uM 2-AA, the differences of other treatments to control are not statistically significant. This increase in coupling efficiency could be a potential method the cells are using to increase their mitochondrial activity.

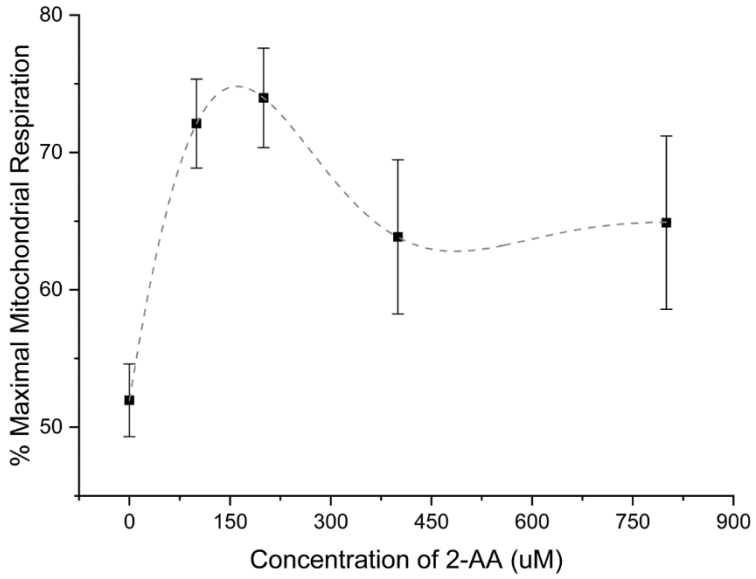

Figure 12: Basal Mitochondrial Respiration as a percentage of Maximal Mitochondrial Respiration for treated RAW cells

Basal mitochondrial respiration is expressed as a percentage of maximal mitochondrial respiration. Error is +/- SEM, n=3.

Two modes of activity occur in this test as concentration of 2-AA is increased. Between 0uM and 100uM, basal mitochondrial respiration increased ~40%. At concentrations below 200uM, 2-AA has an activating effect on mitochondrial respiration. At concentrations beyond this point, usage decreases ~13%, and no change is seen between 400uM and 800uM.

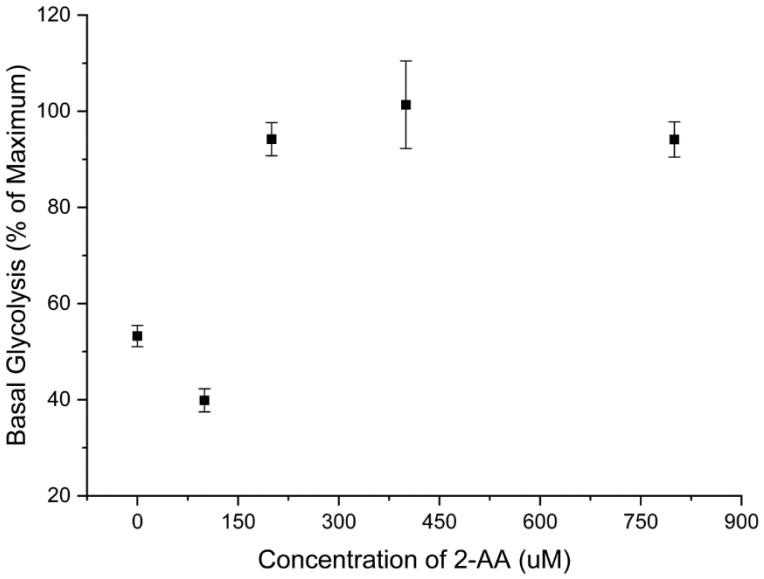

Figure 13: Basal Glycolysis as a percentage of Maximal Glycolysis for treated RAW cells

A decrease of ~27% is seen in basal glycolysis from control to 100uM 2-AA incubation. Then a ~130% increase is seen from 100uM 2-AA to 200uM 2-AA. No changes are seen from 200uM to 800uM, and all three are above 90% usage of total maximum glycolysis. Error is +/- SEM, n=3.

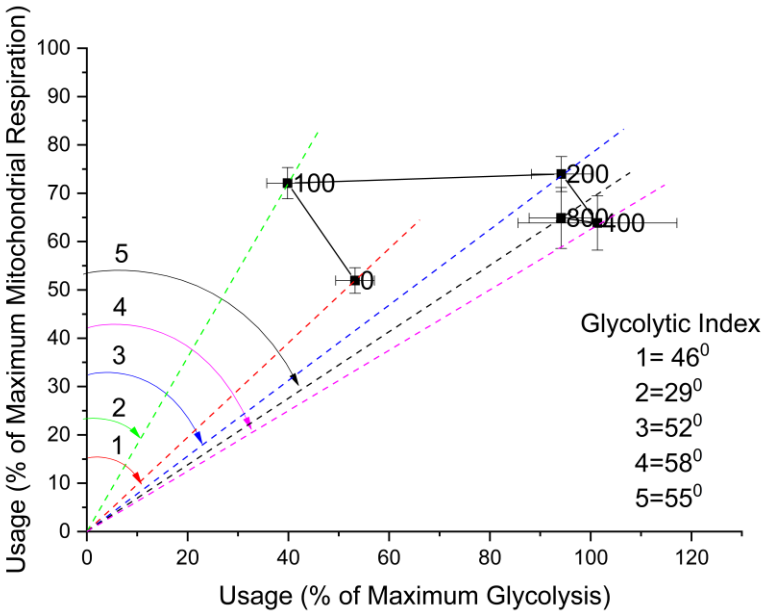

Figure 14: Glycolytic Index of 2-AA treated RAW cells

Glycolytic Index (GI) is a method used to describe how reliant a given cell is on glycolysis. Higher angle indicates higher reliance on glycolysis as a source for energy as opposed to mitochondrial respiration. Error is +/- SEM, n=3.

A shift of -17º is seen between cells incubated in 0uM 2-AA and those incubated in 100uM 2-AA. The cells in the 100uM condition are favoring mitochondrial respiration more than cells in the 0uM condition. A shift of 23º is seen between 100uM and 200uM, indicating a shift back towards glycolysis. The shifts between 200uM and 800uM are fairly small and the differences may be non-significant.

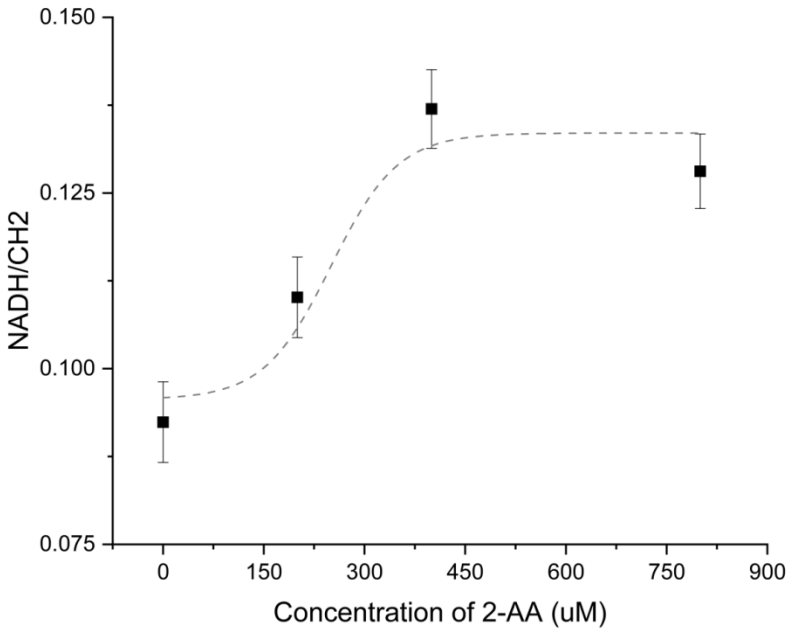

Figure 15: Ratio of NADH peak to CH_2 for treated RAW cells

The ratios of NADH (1590cm^{-1}) to CH_2 (2940cm^{-1}) were calculated for each concentration of 2-AA. The association between NADH and the 1590cm^{-1} peak was established by direct scans of pure NADH. The association between CH_2 and the 2940cm^{-1} peak has been previously established (Bellamy, 1975). Error is +/- SEM, n=3.

The ratio of the intensity of the NADH peak to the intensity of the CH_2 peak is increasing between 0uM and 400uM. From 0uM to 200uM, an increase of ~19% was seen. Between 200uM and 400uM, a ~24% increase is seen.

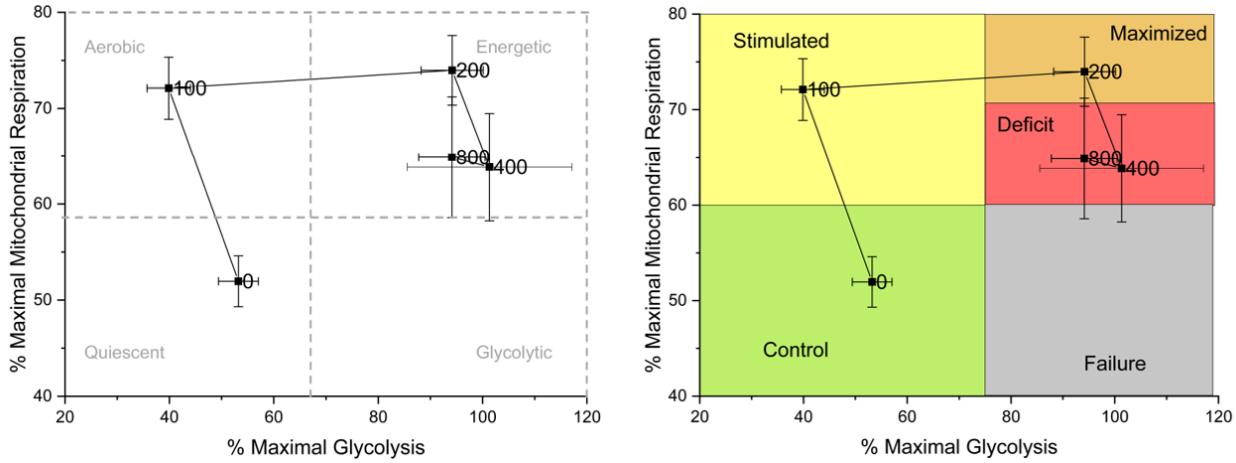

Figure 16: Cell Phenotype Analysis Matrix for RAW cells treated with 2-AA

For each condition, Basal Respiration and Basal Glycolysis are each plotted as a percentage of Maximal Respiration and Maximal Glycolysis, respectively. Error is +/- SEM, n=3.

Metabolic regions are overlaid on the left. Descriptive and predictive regions are shown on the right. Descriptive and predictive regions are generated with knowledge of the changing concentration of NADH in mind.

Discussion

In Figure 11, the coupling efficiency is fitted with a sine dampening curve (R^2=0.992). Coupling efficiency increases from 0uM to 100uM, but then decreases back to control levels for 400uM and 800uM. The Pasteur shift towards mitochondrial respiration from 0uM to 100uM seen in Figure 14 could be due to this increase in coupling efficiency.

Mitochondrial ATP production as a percentage of total ATP production forms a parabolic curve (R^2=0.998), where a simulative effect is seen on mitochondrial ATP production, then a

depressive effect is seen at higher concentrations of 2-AA. The stimulation aligns with previous work done on *in vivo* effects of 2-AA (Bandyopadhaya, 2012; Tzika, 2013).

Due to the two modes of activity seen in Figure 10, the nature of the relationship between RAW macrophages and 2-AA is seen. The data is fit with a sine dampening curve (R^2=0.9999). At 100uM, it produces a stimulating effect on mitochondrial respiration, which when coupled with the slight depressive effect seen on glycolysis, explains the Pasteur shift seen in Figure 12. Increasing concentration of 2-AA to 200uM shows a maximizing effect on the cells, which is best shown in Figure 13. A new energy demand is seen going for 100uM to 200uM, and the cells cope by increasing use of glycolysis. Increasing concentration further to 400uM and 800uM, a decrease from the maximized mitochondrial state is seen. If a hypothetical cell was incubated in a higher concentration, it would appear on the matrix near the failure region, and would be undergoing apoptosis. The descriptive and predictive regions hold true for only this cell line and this condition, but allows for estimation of effect of concentrations between those tested in this study. 2-AA must play a role in lowering mitochondrial efficiency.

NADH is a molecule that transfers electrons from glycolysis and the TCA cycle to the electron transport chain. Energy from those electrons will go on to pump protons across the membrane, which will then generate ATP. As concentration of 2-AA increases beyond ~200uM, suppressive effects are seen on mitochondrial respiration. Paired with a maximization of glycolysis, this indicates a potential breakdown in molecules that couple glycolysis with the electron transport chain, possibly NADH. Using Raman spectroscopy, ratios of NADH to CH were calculated. A Boltzmann curve was fitted to the data (R^2=0.922). These show that the amount of NADH is increased as concentration of 2-AA is increased. The mitochondria are not

able to use these energy molecules as effectively in this case, which could be leading to the suppressive effect. This is similar to the effect seen on mitochondria by Tzika et al.(Tzika 2013)

Conclusion and Further Work

The combination of extracellular flux analysis and Raman spectroscopy allows for a deeper study of metabolism in macrophages treated with 2-AA. This study further confirmed both the stimulation of the mitochondria at low concentrations (<200uM) and the suppression of the mitochondria at high concentrations (>400uM) seen previously. This combination of techniques also offers a potential cause for the suppression of mitochondrial activity as disruption of the ability of NADH to deliver its high energy electrons.

More work will need to be done to determine why the amount of NADH is changing, and what specifically 2-AA is doing to the mitochondria. Further multimodal tests can be done on other quorum sensing molecules, or on metabolites of 2-AA. It is expected that similar trends will be seen in the case of known quorum sensing molecules HHQ and PQS (Kim, 2009). Using this multimodal system, studies of the host-pathogen relationship can be made.

CHAPTER FOUR: CONCLUSION

This multimodal technique, when paired with other non-destructive assays like long-term viability studies, allows for a deeper study of metabolism and overall cell health. Unlike destructive assays, cell dependent and real-time measurements can be made. This multimodal technique can be used for any cell type and any condition, which makes it very versatile.

As seen in chapter 3, once a certain amount of data is collected, large scale trends can be identified. These trends can then be extrapolated to predict metabolic health at conditions beyond the scope of what was studied.

REFERENCES

1. Adler, C. H. (2005). Nonmotor complications in Parkinsons disease. *Movement Disorders, 20*(S11). doi:10.1002/mds.20460

2. Asher, S. A., Ludwig, M., & Johnson, C. R. (1986). UV Resonance Raman excitation profiles of the aromatic amino acids. *Journal of the American Chemical Society, 108*(12), 3186-3197. doi:10.1021/ja00272a005

3. Bandyopadhaya, A., Kesarwani, M., Que, Y., He, J., Padfield, K., Tompkins, R., & Rahme, L. G. (2012). The Quorum Sensing Volatile Molecule 2-Amino Acetophenone Modulates Host Immune Responses in a Manner that Promotes Life with Unwanted Guests. *PLoS Pathogens, 8*(11). doi:10.1371/journal.ppat.1003024

4. Baronti, F., Mouradian, M. M., Conant, K. E., Giuffra, M., Brughitta, G., & Chase, T. N. (1992). Partial dopamine agonist therapy of levodopa-induced dyskinesias. *Neurology, 42*(6), 1241-1241. doi:10.1212/wnl.42.6.1241

5. Basma AN, Morris EJ, Nicklas WJ, Geller HM. L-dopa cytotoxicity to PC12 cells in culture is via its autoxidation. J Neurochem. 1995; 64:825–832. [PubMed: 7830076]

6. Bellamy, L. J. (1975). *The infra-red spectra of complex molecules*. London: Chapman and Hall.

7. Bhat, A. H., Dar, K. B., Anees, S., Zargar, M. A., Masood, A., Sofi, M. A., & Ganie, S. A. (2015). Oxidative stress, mitochondrial dysfunction and neurodegenerative diseases; a mechanistic insight. *Biomedicine & Pharmacotherapy, 74*, 101-110. doi:10.1016/j.biopha.2015.07.025

8. Biswas, S., Hazeldine, S., Ghosh, B., Parrington, I., Kuzhikandathil, E., Reith, M. E., & Dutta, A. K. (2008). Bioisosteric Heterocyclic Versions of 7-{[2-(4-Phenyl-piperazin-1-yl)ethyl]propylamino}-5,6,7,8-tetrahydronaphthalen-2-ol: Identification of Highly Potent and Selective Agonists for Dopamine D3 Receptor with Potent in Vivo Activity. *Journal of Medicinal Chemistry, 51*(10), 3005-3019. doi:10.1021/jm701524h

9. Blum, D., Torch, S., Nissou, M., Benabid, A., & Verna, J. (2000). Extracellular toxicity of 6-hydroxydopamine on PC12 cells. *Neuroscience Letters, 283*(3), 193-196. doi:10.1016/s0304-3940(00)00948-4

10. Blum, D., Torch, S., Lambeng, N., Nissou, M., Benabid, A., Sadoul, R., & Verna, J. (2001). Molecular pathways involved in the neurotoxicity of 6-OHDA, dopamine and MPTP: Contribution to the apoptotic theory in Parkinsons disease. *Progress in Neurobiology, 65*(2), 135-172. doi:10.1016/s0301-0082(01)00003-x

11. Brand, M. (2005). The efficiency and plasticity of mitochondrial energy transduction. *Biochemical Society Transactions, 33*(5), 897-904. doi:10.1042/bst0330897
12. Breese, G. R., Knapp, D. J., Criswell, H. E., Moy, S. S., Papadeas, S. T., & Blake, B. L. (2005). The neonate-6-hydroxydopamine-lesioned rat: A model for clinical neuroscience and neurobiological principles. *Brain Research Reviews, 48*(1), 57-73. doi:10.1016/j.brainresrev.2004.08.004

13. Byrd, J. C., Hadjiconstantinou, M., & Cavalla, D. (1986). Epinephrine synthesis in the PC12 pheochromocytoma cell line. *European Journal of Pharmacology, 127*(1-2), 139-142. doi:10.1016/0014-2999(86)90216-5

14. Cadenas, E., & Davies, K. J. (2000). Mitochondrial free radical generation, oxidative stress, and aging. *Free Radical Biology and Medicine, 29*(3-4), 222-230. doi:10.1016/s0891-5849(00)00317-8

15. Chazotte, B. (2011). Labeling Mitochondria with MitoTracker Dyes. *Cold Spring Harbor Protocols, 2011*(8). doi:10.1101/pdb.prot5648

16. Cohen, G., Farooqui, R., & Kesler, N. (1997). Parkinson Disease: A New Link between Monoamine Oxidase and Mitochondrial Electron Flow. *Proceedings of the National Academy of Sciences of the United States of America, 94*(10), 4890-4894. Retrieved from http://0-www.jstor.org.wizard.umd.umich.edu/stable/42419

17. Cystic Fibrosis Foundation. (2017). *2016 Patient Registry Annual Data Report*. Bethesda, MD: Cystic Fibrosis Foundation.

18. Depietro, F. R., & Fernstrom, J. D. (1999). The relative roles of phenylalanine and tyrosine as substrates for DOPA synthesis in PC12 cells. *Brain Research, 831*(1-2), 72-84. doi:10.1016/s0006-8993(99)01400-6

19. Drees, S., & Fetzner, S. (2015). PqsE of Pseudomonas aeruginosa Acts as Pathway-Specific Thioesterase in the Biosynthesis of Alkylquinolone Signaling Molecules. *Chemistry & Biology, 22*(5), 611-618. doi:10.1016/j.chembiol.2015.04.012

20. Ebert, S. N., Lindley, S. E., Bengoechea, T. G., Bain, D., & Wong, D. L. (1997). Adrenergic differentiation potential in PC12 cells: Influence of sodium butyrate and dexamethasone. *Molecular Brain Research, 47*(1-2), 24-30. doi:10.1016/s0169-328x(97)00032-6

21. Fahn, S., & Cohen, G. (1992). The oxidant stress hypothesis in Parkinsons disease: Evidence supporting it. *Annals of Neurology, 32*(6), 804-812. doi:10.1002/ana.410320616

22. Fearnley, J. M., & Lees, A. J. (1991). Ageing And Parkinsons Disease: Substantia Nigra Regional Selectivity. *Brain, 114*(5), 2283-2301. doi:10.1093/brain/114.5.2283

23. Fulda, S. (2014). Cross Talk Between Cell Death Regulation and Metabolism. *Methods in Enzymology Conceptual Background and Bioenergetic/Mitochondrial Aspects of Oncometabolism,* 81-90. doi:10.1016/b978-0-12-416618-9.00004-2

24. Gee, P., & Davison, A. (1989). Intermediates in the aerobic autoxidation of 6-hydroxydopamine: Relative importance under different reaction conditions. *Free Radical Biology and Medicine, 6*(3), 271-284. doi:10.1016/0891-5849(89)90054-3

25. Giordano, S., Lee, J., Darley-Usmar, V., & Zhang, J. (2012). Distinct effects of rotenone, 1-methyl-4-phenylpyridinium and 6-hydroxydopamine on cellular bioenergetics and cell death. *PLoS One, 7*(9) doi:http://dx.doi.org/10.1371/journal.pone.0044610

26. Glennon, J. C., Scharrenburg, G. V., Ronken, E., Hesselink, M. B., Reinders, J., Neut, M. V., . . . Mccreary, A. C. (2006). In vitro characterization of SLV308 (7-[4-methyl-1-piperazinyl]-2(3H)-benzoxazolone, monohydrochloride): A novel partial dopamine D2 and D3 receptor agonist and serotonin 5-HT1A receptor agonist. *Synapse, 60*(8), 599-608. doi:10.1002/syn.20330

27. Gogoi, S. , Antonio, T. , Rajagopalan, S. , Reith, M. , Andersen, J. and Dutta, A. K. (2011), Dopamine D_2/D_3 Agonists with Potent Iron Chelation, Antioxidant and Neuroprotective Properties: Potential Implication in Symptomatic and Neuroprotective Treatment of Parkinson's Disease. ChemMedChem, 6: 991-995. doi:10.1002/cmdc.201100140

28. Greene, L. A., & Tischler, A. S. (1982). PC12 Pheochromocytoma Cultures in Neurobiological Research. *Advances in Cellular Neurobiology,* 373-414. doi:10.1016/b978-0-12-008303-9.50016-5

29. Hanrott, K., Gudmunsen, L., Oneill, M. J., & Wonnacott, S. (2005). 6-Hydroxydopamine-induced Apoptosis Is Mediated via Extracellular Auto-oxidation and Caspase 3-dependent Activation of Protein Kinase Cδ. *Journal of Biological Chemistry, 281*(9), 5373-5382. doi:10.1074/jbc.m511560200

30. Hartley, A., Stone, J. M., Heron, C., Cooper, J. M., & Schapira, A. H. (2002). Complex I Inhibitors Induce Dose-Dependent Apoptosis in PC12 Cells: Relevance to Parkinsons Disease. *Journal of Neurochemistry, 63*(5), 1987-1990. doi:10.1046/j.1471-4159.1994.63051987.x

31. Hastings, T. G., Lewis, D. A., & Zigmond, M. J. (1996). Role of oxidation in the neurotoxic effects of intrastriatal dopamine injections. *Proceedings of the National Academy of Sciences, 93*(5), 1956-1961. doi:10.1073/pnas.93.5.1956

32. James, P. E., Jackson, S. K., Grinberg, O. Y., & Swartz, H. M. (1995). The effects of endotoxin on oxygen consumption of various cell types in vitro: An EPR oximetry study. *Free Radical Biology and Medicine, 18*(4), 641-647. doi:10.1016/0891-5849(94)00179-n

33. Johnson, M., Antonio, T., Reith, M. E., & Dutta, A. K. (2012). Structure–Activity Relationship Study of N6-(2-(4-(1H-Indol-5-yl)piperazin-1-yl)ethyl)-N6-propyl-4,5,6,7-tetrahydrobenzo[d]thiazole-2,6-diamine Analogues: Development of Highly Selective D3 Dopamine Receptor Agonists along with a Highly Potent D2/D3 Agonist and Their Pharmacological Characterization. *Journal of Medicinal Chemistry,55*(12), 5826-5840. doi:10.1021/jm300268s

34. Jones, C., Johnston, L., Jackson, M., Smith, L., Scharrenburg, G. V., Rose, S., . . . Mccreary, A. (2010). An in vivo pharmacological evaluation of pardoprunox (SLV308) — A novel combined dopamine D2/D3 receptor partial agonist and 5-HT1A receptor agonist with efficacy in experimental models of Parkinsons disease. *European Neuropsychopharmacology, 20*(8), 582-593. doi:10.1016/j.euroneuro.2010.03.001

35. Joyce, J., & Millan, M. (2007). Dopamine D3 receptor agonists for protection and repair in Parkinsons disease. *Current Opinion in Pharmacology, 7*(1), 100-105. doi:10.1016/j.coph.2006.11.004

36. Kadenbach, B., Kuhn-Nentwig, L., & Büge, U. (1987). Evolution of a Regulatory Enzyme: Cytochrome-c Oxidase (Complex IV). *Current Topics in Bioenergetics - Structure, Biogenesis, and Assembly of Energy Transducing Enzyme Systems Current Topics in Bioenergetics,* 113-161. doi:10.1016/b978-0-12-152515-6.50009-6

37. Kim, K., Kim, Y. U., Koh, B. H., Hwang, S. S., Kim, S., Lépine, F., . . . Lee, G. R. (2009). HHQ and PQS, two Pseudomonas aeruginosa quorum-sensing molecules, down-regulate the innate immune responses through the nuclear factor-κB pathway. *Immunology, 129*(4), 578-588. doi:10.1111/j.1365-2567.2009.03160.x

38. Lee, H. I., Kim, M. S., & Suh, S. W. (1989). ChemInform Abstract: Raman Spectroscopy of L-Phenylalanine, L-Tyrosine, and Their Peptides Adsorbed on Silver Surface. *ChemInform, 20*(8). doi:10.1002/chin.198908299

39. Linert, W., & Jameson, G. (2000). Redox reactions of neurotransmitters possibly involved in the progression of Parkinsons Disease. *Journal of Inorganic Biochemistry, 79*(1-4), 319-326. doi:10.1016/s0162-0134(99)00238-x

40. Lotharius, J., & Brundin, P. (2002). Pathogenesis of parkinsons disease: Dopamine, vesicles and α-synuclein. *Nature Reviews Neuroscience, 3*(12), 932-942. doi:10.1038/nrn983

41. Michel, P., Hirsch, E., & Hunot, S. (2016). Understanding Dopaminergic Cell Death Pathways in Parkinson Disease. *Neuron, 90*(4), 675-691. doi:10.1016/j.neuron.2016.03.038

42. Millan, M. J. (2010). From the cell to the clinic: A comparative review of the partial D2/D3 receptor agonist and α2-adrenoceptor antagonist, piribedil, in the treatment of Parkinsons disease. *Pharmacology & Therapeutics, 128*(2), 229-273. doi:10.1016/j.pharmthera.2010.06.002

43. Miller, M. B., & Bassler, B. L. (2001). Quorum sensing in bacteria. *Annual Review of Microbiology, 55*, 165-199. doi:10.1146/annurev.micro.55.1.165

44. Mo, M. L., Palsson, B. Ø, & Herrgård, M. J. (2009). Connecting extracellular metabolomic measurements to intracellular flux states in yeast. *BMC Systems Biology, 3*(1), 37. doi:10.1186/1752-0509-3-37

45. Mookerjee, S. A., Gerencser, A. A., Nicholls, D. G., & Brand, M. D. (2018). Quantifying intracellular rates of glycolytic and oxidative ATP production and consumption using extracellular flux measurements. *Journal of Biological Chemistry, 293*(32), 12649-12652. doi:10.1074/jbc.aac118.004855

46. Moura, M. B., & Houten, B. V. (2014). Bioenergetic Analysis of Intact Mammalian Cells Using the Seahorse XF24 Extracellular Flux Analyzer and a Luciferase ATP Assay. *Molecular Toxicology Protocols Methods in Molecular Biology,* 589-602. doi:10.1007/978-1-62703-739-6_40

47. Neves, S. R. (2002). G Protein Pathways. *Science, 296*(5573), 1636-1639. doi:10.1126/science.1071550

48. Oliver, A., Canton, R., Campo, P., Baquero, F., & Blasquez, J. (2000). High Frequency of Hypermutable Pseudomonas aeruginosa in Cystic Fibrosis Lung Infection. *Science, 288*(5469), 1251-1253. doi:10.1126/science.288.5469.1251

49. Orrenius, S., Gogvadze, V., & Zhivotovsky, B. (2007). Mitochondrial Oxidative Stress: Implications for Cell Death. *Annual Review of Pharmacology and Toxicology, 47*(1), 143-183. doi:10.1146/annurev.pharmtox.47.120505.105122

50. Ott, M., Gogvadze, V., Orrenius, S., & Zhivotovsky, B. (2007). Mitochondria, oxidative stress and cell death. *Apoptosis, 12*(5), 913-922. doi:10.1007/s10495-007-0756-2

51. Parsek, M. R., & Greenberg, E. P. (1999). [3] Quorum sensing signals in development of Pseudomonas aeruginosa biofilms. *Biofilms Methods in Enzymology,* 43-55. doi:10.1016/s0076-6879(99)10005-3

52. Patergnani, S., Baldassari, F., Marchi, E. D., Karkucinska-Wieckowska, A., Wieckowski, M. R., & Pinton, P. (2014). Methods to Monitor and Compare Mitochondrial and Glycolytic ATP Production. *Methods in Enzymology Conceptual Background and Bioenergetic/Mitochondrial Aspects of Oncometabolism,* 313-332. doi:10.1016/b978-0-12-416618-9.00016-9

53. Pelletier, M., Billingham, L. K., Ramaswamy, M., & Siegel, R. M. (2014). Extracellular Flux Analysis to Monitor Glycolytic Rates and Mitochondrial Oxygen Consumption. *Methods in Enzymology Conceptual Background and Bioenergetic/Mitochondrial Aspects of Oncometabolism,* 125-149. doi:10.1016/b978-0-12-416618-9.00007-8

54. Pires, A., & Hadfield, M. G. (1992). Oxidative Breakdown Products of Catecholamines and Hydrogen Peroxide Induce Partial Metamorphosis in the Nudibranch Phestilla sibogae Bergh (Gastropoda: Opisthobranchia). *Biological Bulletin, 182*(1), Iv. doi:10.2307/1542174

55. Porter, A. G., & Jänicke, R. U. (1999). Emerging roles of caspase-3 in apoptosis. *Cell Death & Differentiation, 6*(2), 99-104. doi:10.1038/sj.cdd.4400476

56. Saito, Y., Nishio, K., Ogawa, Y., Kinumi, T., Yoshida, Y., Masuo, Y., & Niki, E. (2007). Molecular mechanisms of 6-hydroxydopamine-induced cytotoxicity in PC12 cells: Involvement of hydrogen peroxide-dependent and -independent action. *Free Radical Biology and Medicine, 42*(5), 675-685. doi:10.1016/j.freeradbiomed.2006.12.004

57. Sciacovelli, M., Gaude, E., Hilvo, M., & Frezza, C. (2014). The Metabolic Alterations of Cancer Cells. *Methods in Enzymology Conceptual Background and Bioenergetic/Mitochondrial Aspects of Oncometabolism,* 1-23. doi:10.1016/b978-0-12-416618-9.00001-7

58. Scott-Thomas AJ, Syhre M, Pattemore PK, Epton M, Laing R, et al. (2010) 2-Aminoacetophenone as a potential breath biomarker for Pseudomonas aeruginosa in the cystic fibrosis lung. BMC Pulm Med 10: 56.

59. Shafer TJ, Atchison WD. Transmitter, ion channel and receptor properties of pheochromocytoma (PC12) cells: a model for neurotoxicological studies. Neurotoxicology. 1991;12(3) 473-492. PMID: 1720882.

60. Shah, M., Rajagopalan, S., Xu, L., Voshavar, C., Shurubor, Y., Beal, F., . . . Dutta, A. K. (2014). The high-affinity D2/D3 agonist D512 protects PC12 cells from 6-OHDA-induced apoptotic cell death and rescues dopaminergic neurons in the MPTP mouse model of Parkinsons disease. *Journal of Neurochemistry, 131*(1), 74-85. doi:10.1111/jnc.12767

61. Simonnet, H., Vigneron, A., & Pouysségur, J. (2014). Conventional Techniques to Monitor Mitochondrial Oxygen Consumption. *Methods in Enzymology Conceptual Background and Bioenergetic/Mitochondrial Aspects of Oncometabolism,* 151-161. doi:10.1016/b978-0-12-416618-9.00008-x

62. Singh, S., & Dikshit, M. (2007). Apoptotic neuronal death in Parkinsons disease: Involvement of nitric oxide. *Brain Research Reviews, 54*(2), 233-250. doi:10.1016/j.brainresrev.2007.02.001

63. Staveley, L. A. (2016). *The Characterization of Chemical Purity: Organic Compounds*.

64. Teslaa, T., & Teitell, M. A. (2014). Techniques to Monitor Glycolysis. *Methods in Enzymology Conceptual Background and Bioenergetic/Mitochondrial Aspects of Oncometabolism,* 91-114. doi:10.1016/b978-0-12-416618-9.00005-4

65. Tzika, A. A., Constantinou, C., Bandyopadhaya, A., Psychogios, N., Lee, S., Mindrinos, M., . . . Rahme, L. G. (2013). A Small Volatile Bacterial Molecule Triggers Mitochondrial Dysfunction in Murine Skeletal Muscle. *PLoS ONE, 8*(9). doi:10.1371/journal.pone.0074528

66. Usiello, A., Baik, J., Rougé-Pont, F., Picetti, R., Dierich, A., Lemeur, M., . . . Borrelli, E. (2000). Distinct functions of the two isoforms of dopamine D2 receptors. *Nature, 408*(6809), 199-203. doi:10.1038/35041572

67. Wang C, Youle RJ. The role of mitochondria in apoptosis*. *Annu Rev Genet*. 2009;43:95–118. doi:10.1146/annurev-genet-102108-134850

68. Wang, X., Li, J., Dong, G., & Yue, J. (2014). The endogenous substrates of brain CYP2D. *European Journal of Pharmacology, 724*, 211-218. doi:10.1016/j.ejphar.2013.12.025

69. Whiteley, M., Bangera, M. G., Bumgarner, R. E., Parsek, M. R., Teitzel, G. M., Lory, S., & Greenberg, E. P. (2001). Gene expression in Pseudomonas aeruginosa biofilms. *Nature, 413*(6858), 860-864. doi:10.1038/35101627

70. Wu, Y., Blum, D., Nissou, M., Benabid, A., & Verna, J. (1996). Unlike MPP , apoptosis induced by 6-OHDA in PC12 cells is independent of mitochondrial inhibition. *Neuroscience Letters, 221*(1), 69-71. doi:10.1016/s0304-3940(96)13276-6

71. Zhang, J., & Darley-Usmar, V. (2011). Mitochondrial Dysfunction in Neurodegenerative Disease: Protein Aggregation, Autophagy, and Oxidative Stress. *Mitochondrial Dysfunction in Neurodegenerative Disorders,* 95-111. doi:10.1007/978-0-85729-701-3_6

APPENDIX I: SUPPLEMENTAL FIGURES

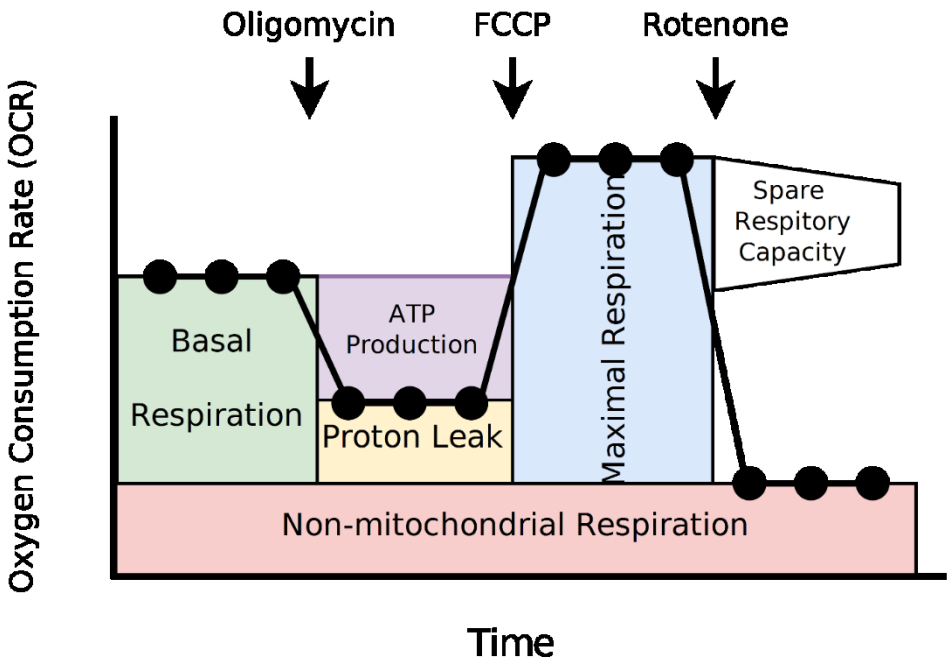

Figure 17: Sample Illustration of a Typical Mitochondrial Stress Test

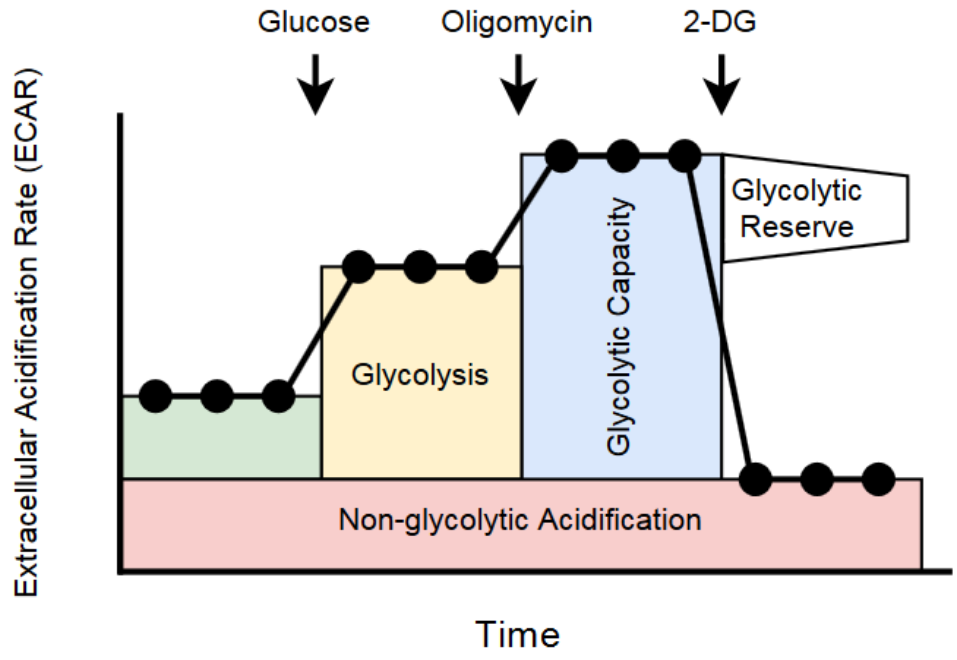

Figure 18: Sample Illustration of a Typical Glycolytic Stress Test

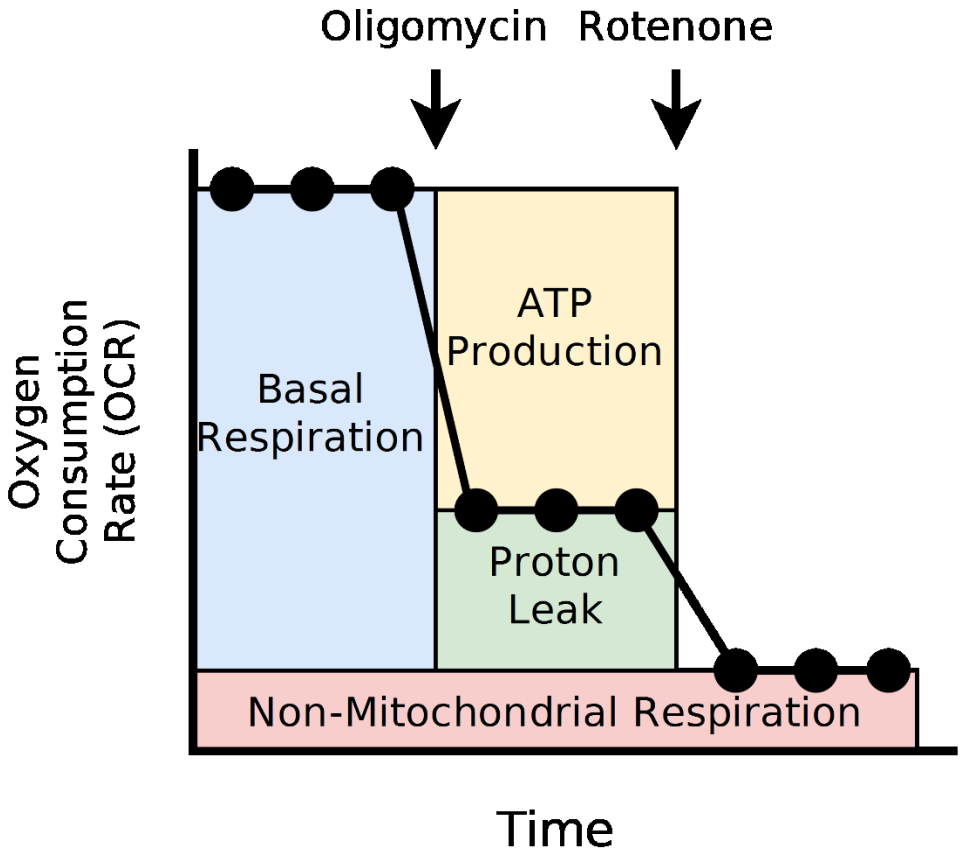

Figure 19: Sample Illustration of a Typical Real-Time ATP Assay

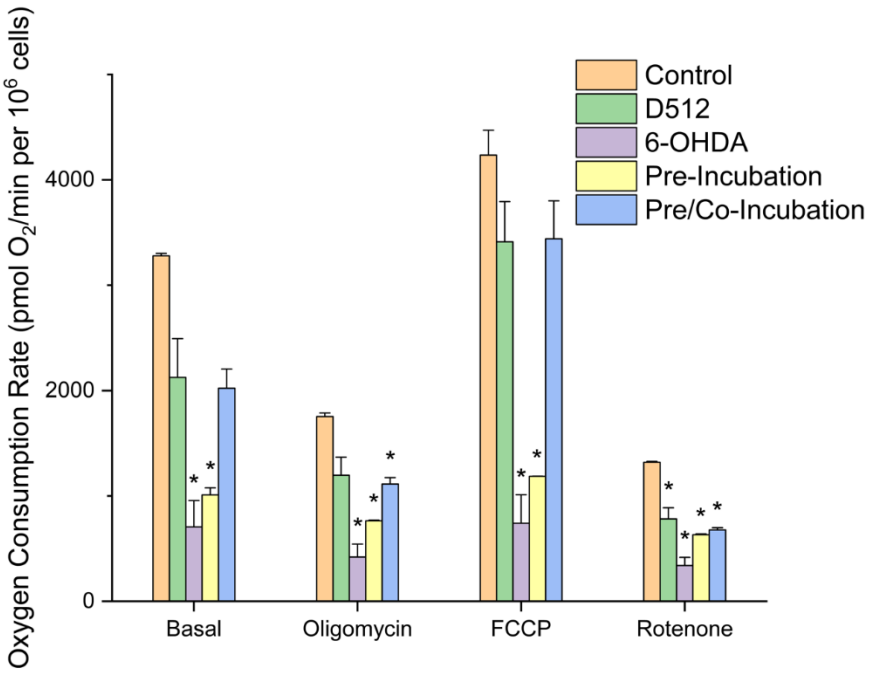

Figure 20: Measurement of OCR of treated PC-12 during Mito Stress Test

*<0.05 against control. Error is +/- SEM, n=3.

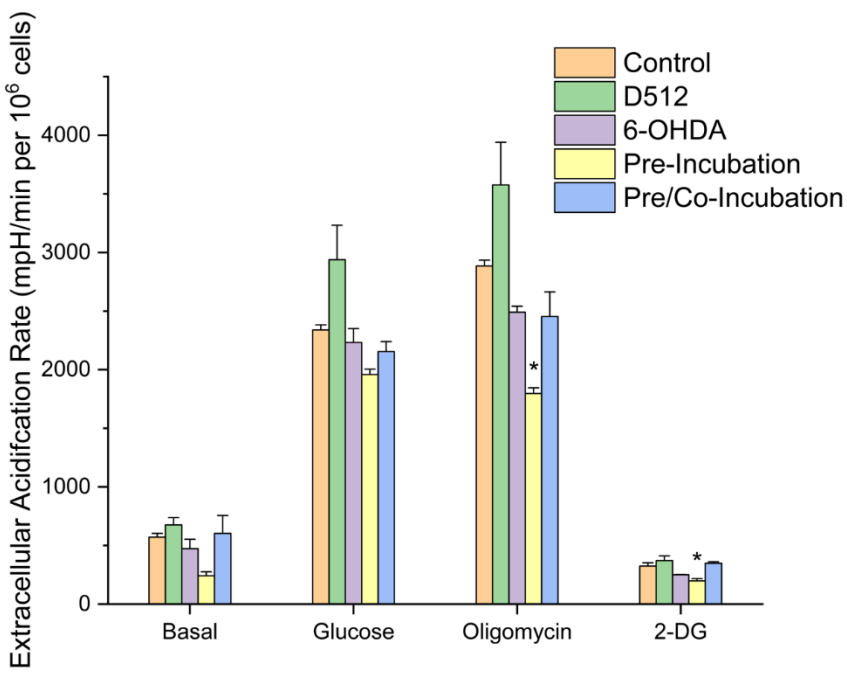

Figure 21: Measurement of ECAR of treated PC-12 during Glyco Stress Test

*<0.05 against control. Error is +/- SEM, n=3.

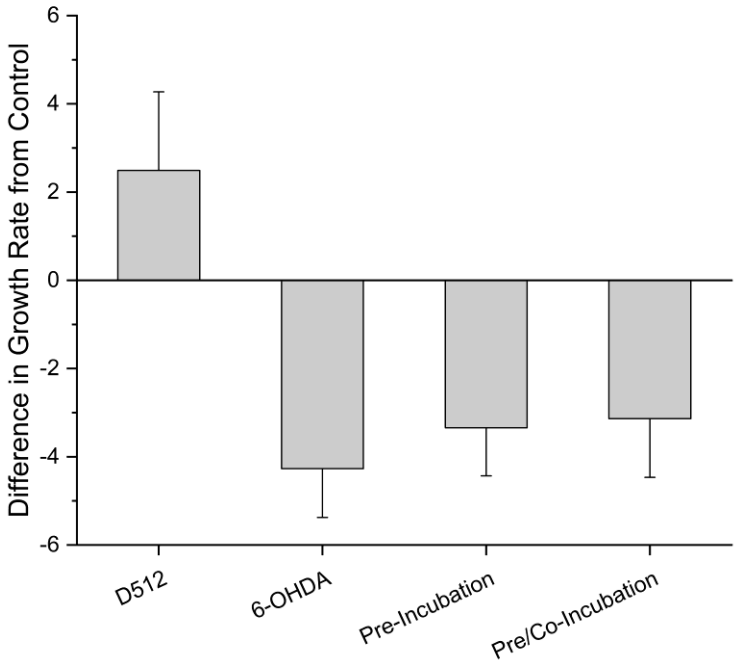

Figure 22: Difference in Growth Rate from Control in treated PC-12

Using normalized growth rates from Figure 4, control rate was subtracted from the growth rates of the treated cells. Error is +/- SEM, n=4.

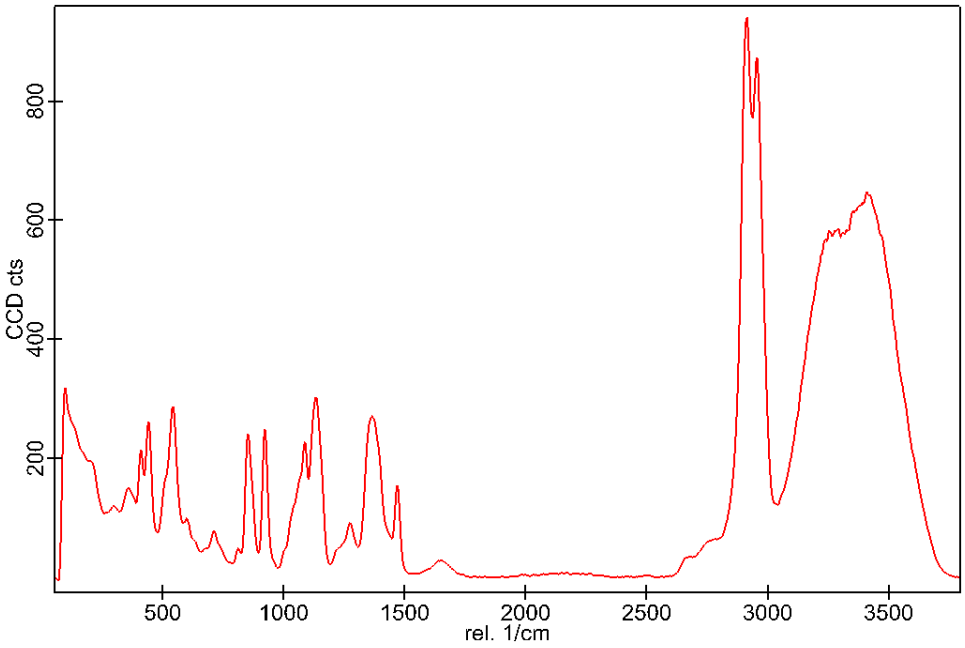

Figure 23: Sample Raman Spectrum of Trehalose in Water

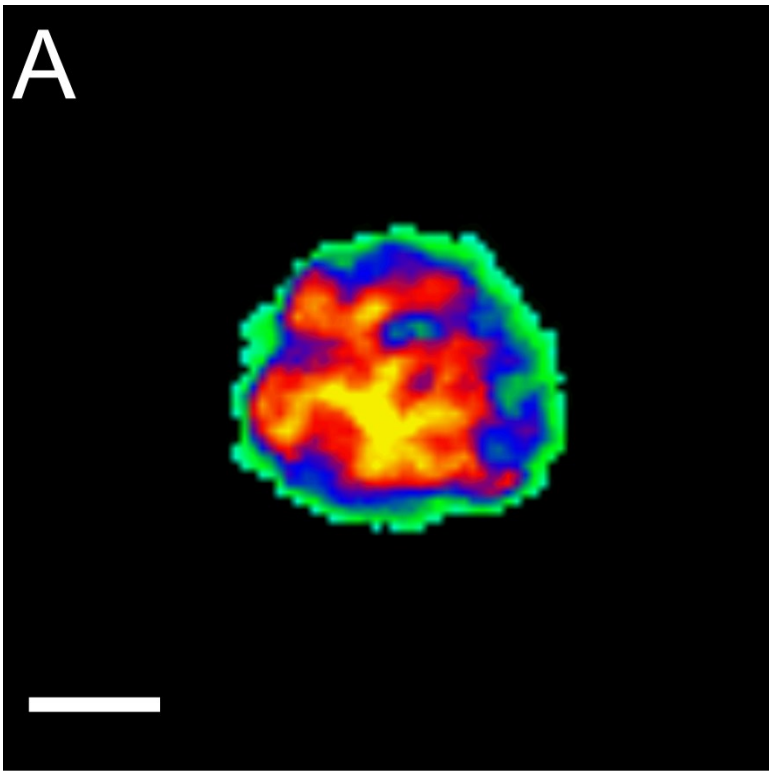

Figure 24: Hyperspectral Image of a PC-12 cell

The hyperspectral map was generated using total signal. The dimensions of the scan are 20um by 20um. Extracellular regions are set as zero. The bright yellow region most likely encompasses the nucleus of the cell and the surrounding area.

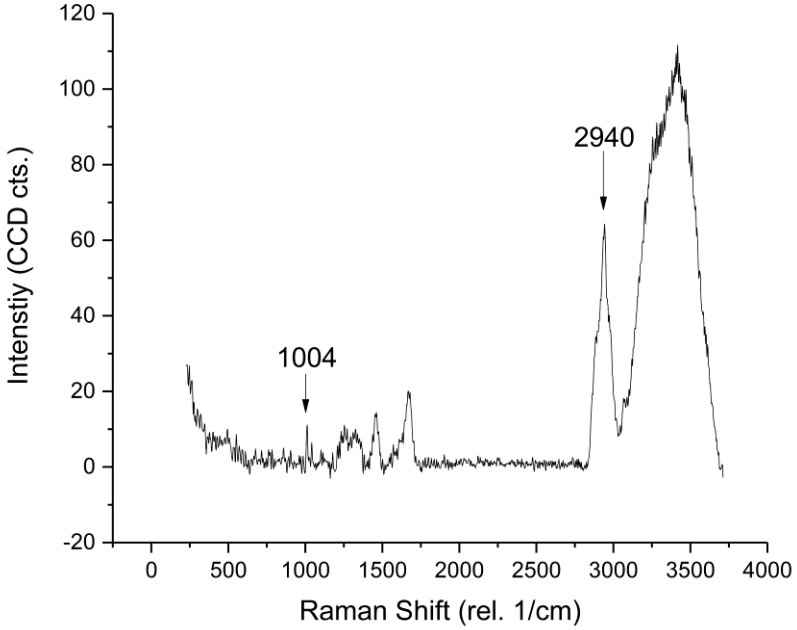

Figure 25: Single point Raman spectrum of a PC-12 cell

Phenylalanine (1004cm^{-1}) and CH_2 (2940cm^{-1}) are labeled.